JOURNAL OF GEOPHYSICAL RESEARCH, VOL. 115, A07227, doi:10.1029/2009JA015104, 2010

IMAGE and DMSP observations of a density trough inside the plasmasphere

H. S. Fu,[1,2,3] J. Tu,[1] J. B. Cao,[2] P. Song,[1] B. W. Reinisch,[1] D. L. Gallagher,[4] and B. Yang[1,5]

Received 17 November 2009; revised 27 February 2010; accepted 15 March 2010; published 27 July 2010.

[1] We report coordinated observations of a density trough within the plasmasphere using the measurements from the radio plasma imager (RPI) and extreme ultraviolet imager (EUV) on the IMAGE satellite and the measurements from DMSP F-15. The density trough inside the plasmasphere with a width of ~0.7 R_E in terms of L shell (from $L \sim 2.3$ to $L \sim 3.0$) was observed in situ by RPI when IMAGE traversed the plasmasphere in ~2130 magnetic local time (MLT) sector. The plasmasphere images taken by the IMAGE EUV instrument confirm that the density trough is inside the plasmasphere. A 2-D electron density image constructed from the RPI active sounding measurements reveals that the density trough extends along the magnetic field from the IMAGE orbit to at least 41° magnetic latitude. Meanwhile, the DMSP-F15 satellite, circling the Earth at about 850 km altitude, detected a light ion density trough at the same time on the same L shells and similar MLT sector. The coordinated observations with the IMAGE and DMSP-F15 satellite demonstrate, for the first time, that the density trough is a low-density plasmaspheric structure extending from the plasmasphere to the topside ionosphere along the geomagnetic field lines.

Citation: Fu, H. S., J. Tu, J. B. Cao, P. Song, B. W. Reinisch, D. L. Gallagher, and B. Yang (2010), IMAGE and DMSP observations of a density trough inside the plasmasphere, *J. Geophys. Res.*, *115*, A07227, doi:10.1029/2009JA015104.

1. Introduction

[2] The dynamics of Earth's plasmasphere is controlled by three types of large-scale processes, namely the magnetospheric convection, the eastward corotation with the Earth, and the coupling between the plasmasphere and the ionosphere [e.g., *Nishida*, 1966; *Carpenter et al.*, 2000]. The variations in these three processes and their interplays lead to large-scale variations of the plasmasphere density distributions in space and time [*Dandouras et al.*, 2009; *Fu et al.*, 2010]. Other localized processes, such as the subauroral ion drift (SAID) [e.g., *De Keyser et al.*, 1998; *Burke et al.*, 2000; *Anderson et al.*, 2001] and various wave activities [e.g., *Moldwin*, 1997; *Adrian et al.*, 2004; *Cao et al.*, 2005], may be responsible for smaller-scale temporal density variations and fine spatial structures. Some density structures, such as plasmaspheric plumes, channels, and troughs, have been inferred from early in situ observations [*Lemaire and Gringauz*, 1998, and references therein]. Other density structures like notches, shoulders, and fingers, however, were not revealed until the recent imaging observations by the extreme ultraviolet imager (EUV) instrument [*Sandel et al.*, 2000] onboard the IMAGE satellite [*Burch et al.*, 2001]. The IMAGE EUV snapshots provided global views and unprecedented details of all those structures [*Sandel et al.*, 2001, 2003; *Burch et al.*, 2001; *Darrouzet et al.*, 2009]. There remain, however, many outstanding questions about those density structures.

[3] In the present study, we focus on the density trough inside the plasmasphere. The density trough is a structure with significantly lower density inside compared to that in the surrounding region, and it exists usually in the aftermath of high geomagnetic activities [e.g., *Horwitz et al.*, 1990; *Carpenter and Lemaire*, 1997]. Several forms of the density trough have been reported previously. For example, *Taylor et al.* [1971] observed such a structure by analyzing the data from the OGO 4 ion composition experiment. They gave a schematic illustration on the equatorial plane and suggested that the density trough results from the corotation effect of a plasma tail or elongation of the plasmasphere. Actually what they observed corresponds to the channel, a region of low-density cold plasma between the main plasmasphere and the region nowadays referred to as the plasmaspheric plume [e.g., *Burch et al.*, 2001]. *Carpenter et al.* [2000] showed a case of the density trough inside the plasmasphere observed by the ISEE1 satellite on the duskside of the plasmasphere at 1700–1900 magnetic local time (MLT) on 17 September 1983. They then analyzed in detail several cases and conducted a statistical study using the data from the CRRES satellite that encircled the Earth in near-equatorial orbits. The properties of the inner density trough have been described by the occurrence rate (~13% of total passes), L shell range ($L < 4$ and $\Delta L = 0.5$–1.5), occurrence in MLT (most in the nighttime),

[1]Center for Atmospheric Research, University of Massachusetts Lowell, Lowell, Massachusetts, USA.
[2]State Key Laboratory for Space Weather/CSSAR, Beijing, China.
[3]Graduate University, Chinese Academy of Sciences, Beijing, China.
[4]NASA Marshall Space Flight Center, Huntsville, Alabama, USA.
[5]Institute of Space Physics and Applied Technology, Peking University, Beijing, China.

0148-0227/10/2009JA015104

duration (up to 10 h or more), and extent in longitude (at least 20°) [*Carpenter et al.*, 2000]. *Horwitz et al.* [1990] performed a statistical study of plasmaspheric density profiles along the Dynamics Explorer 1 orbits measured by the retarding ion mass spectrometers (RIMS). They classified density profiles of the plasmasphere into six categories that include (1) featureless, (2) featureless with enhancement, (3) multiple plateaus, (4) featureless with trough, (5) multiple plateaus with trough, and (6) other complex structures. Among them types (4) and (5) display the density troughs inside the plasmasphere, which tend to occur during high magnetic activities in terms of K_p values and are about 18% (types 4 and 5 in total) of the orbits studied. *Ober et al.* [1997] suggested that the inner density trough was caused by the subauroral ion drift (SAID). They successfully simulated the formation of the troughs by using the dynamic global core plasma model (DGCPM) imposed with a SAID electric field. During the process, the low-density plasma sheet flux tubes convected into the main plasmasphere to form a density trough.

[4] Although a number of studies on the density trough inside the plasmasphere have been conducted, the spatial structures of the density trough, such as the spatial extent of the inner density trough along the geomagnetic fields, are still unknown because the previous density measurements were mainly made locally at the satellite locations [e.g., *Horwitz et al.*, 1990; *Carpenter et al.*, 2000].

[5] In this paper, we present coordinated observations of a density trough embedded inside the plasmasphere using the measurements from IMAGE and DMSP-F15 satellites at magnetospheric and ionospheric altitudes, respectively, on 13 May 2001. The radio plasma imager (RPI) observations on IMAGE allow deriving the field-aligned electron density profiles within the inner density trough for the present case. The extreme ultraviolet (EUV) imager on IMAGE took global images of the plasmasphere. DMSP-F15 provides corresponding observations of this structure at ionosphere altitudes. From the coordinated observations, we determine, for the first time, the spatial extent of the density trough along the geomagnetic field lines.

2. Satellites and Instruments

[6] The IMAGE satellite [*Burch et al.*, 2001] was in a highly elliptical polar orbit with an initial perigee altitude of 1000 km and a geocentric apogee at ~8.22 R_E (Earth radii) so that it passed the plasmasphere down to $L < 2$. In the present study, we use the measurements from the radio plasma imager (RPI) [*Reinisch et al.*, 2000] and the extreme ultraviolet imager (EUV) [*Sandel et al.*, 2000] instruments on board the satellite. RPI operated alternatively between the passive in situ measurements and active sounding measurements for remote sensing of plasma densities. In the passive mode RPI received natural plasma waves usually ranging from 3 to 1100 kHz. The received signals often display an enhanced upper hybrid resonance (UHR) band when the satellite passed the plasmasphere and plasmatrough. The electron density along the spacecraft orbit can be derived from the UHR band because its cutoff frequency is approximately the plasma frequency f_{pe} on the condition that the electron gyrofrequency is significantly lower than the electron plasma frequency [e.g., *Mosier et al.*, 1973], which is usually the case in the plasmasphere and plasmatrough. In the active mode, RPI transmitted coded signals stepping in the range from 3 kHz to 3 MHz and listened to the echoes. Echoes produced by the reflected signals with different frequencies exhibit traces in the plasmagram, a graphic display of the received signal intensities as a function of frequency and echo delay time (represented as virtual range: one half of the echo delay time multiplied by the speed of light in free space). On many occasions the traces formed by the reflected signals resulted from the propagation along the geomagnetic field line that intersected the spacecraft [*Reinisch et al.*, 2001; *Fung and Green*, 2005]. Using such traces, the field-aligned distribution of the electron density can be derived by applying the inversion algorithm developed by *Huang et al.* [2004]. Because the IMAGE orbit covers a wide extent in the magnetosphere where the plasma densities can vary by six orders of magnitude, the flexible measurement programs and schedules are necessary in order to optimize the scientific output of the RPI measurements [*Reinisch et al.*, 2000]. In each measurement program, there are 21 parameters available to control the RPI measurements such as the maximum virtual range. For measurement programs 34 and 35 that are used in this study, the maximum virtual ranges are 8.2 R_E and 4.5 R_E, respectively.

[7] The EUV instrument on the IMAGE satellite provided images of the Earth's plasmasphere with a time resolution of 10 min and a spatial resolution of 0.1 R_E (at apogee) [*Sandel et al.*, 2001]. The EUV consisted of three cameras that captured the emissions at 30.4 nm wavelength coming from the He^+ scattering of the sunlight in the plasmasphere and plasmatrough [*Sandel et al.*, 2000]. The snapshots taken by the three cameras are merged to produce a global image of the He^+ distribution, on which the brightness of each pixel represents the density of He^+ integrated along the line of sight [*Sandel et al.*, 2003]. The EUV obtained global images of the plasmasphere when IMAGE was over the northern or southern polar cap, whereas the RPI measured the plasmasphere density distributions when IMAGE traversed the low and middle latitudes. Thus, there is a time difference of several hours between the EUV and RPI observations of a same structure [e.g., *Reinisch et al.*, 2004].

[8] The Defense Meteorological Satellite Program (DMSP) consists of a constellation of satellites that are in Sun-synchronous polar orbits near 850 km altitude (topside ionosphere) with orbital periods of ~104 min [*Hairston and Heelis*, 1990]. In the present study, we use DMSP-F15 to conduct coordinated observations with the IMAGE satellite because it crossed the local time section similar to that of the IMAGE satellite in the case studied. DMSP-F15 was in an orbit near the 0930–2130 local time meridian. On board the satellite, the RPA instrument measures the ion density, ion compositions, and horizontal component V_x (along the satellite track) of the ion velocity in the range of ±3000 m s^{-1}.

3. Observations

3.1. IMAGE RPI Passive Measurements

[9] Figure 1 displays a dynamic spectrogram obtained by the RPI during the interval of 0430 UT-0730 UT on 13 May 2001, when IMAGE RPI observed a density trough embedded inside the plasmasphere. The small panel on the upper right corner presents IMAGE orbit configuration with the black geomagnetic field lines denoting $L = 4$. As can be seen, during

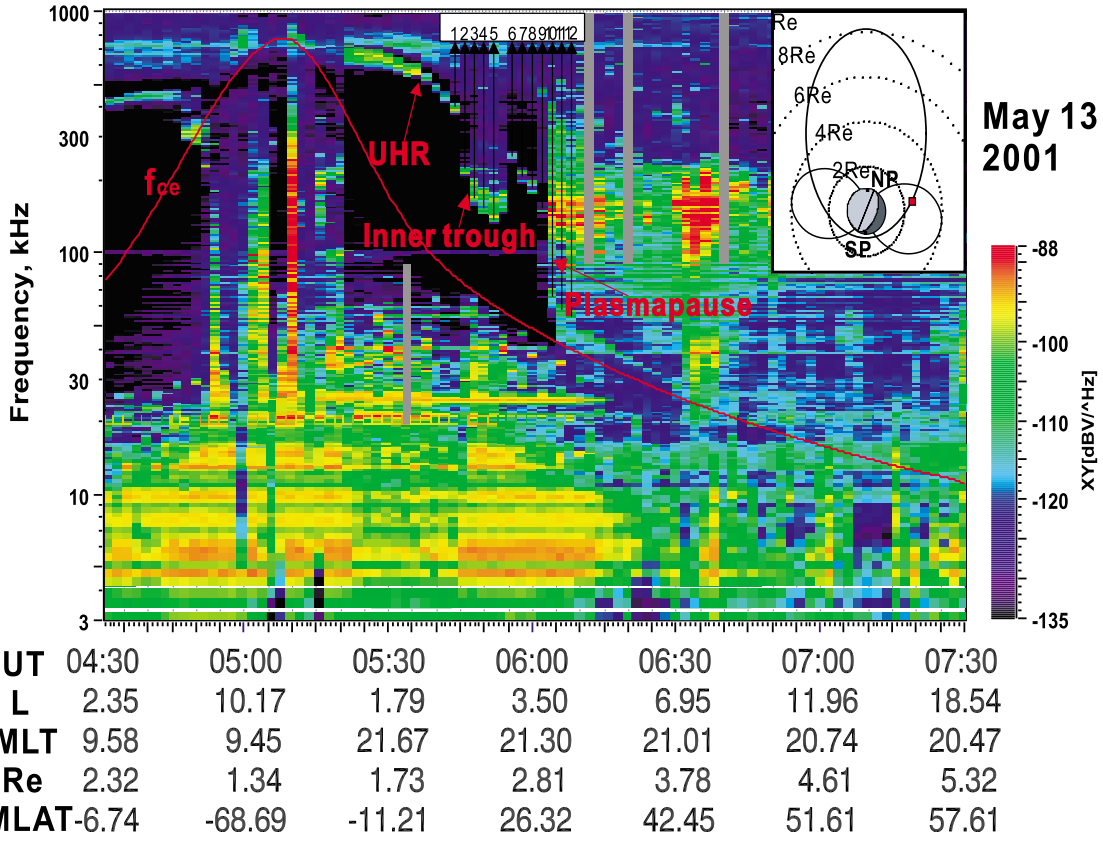

Figure 1. Dynamic spectrogram obtained by the IMAGE RPI passive measurements during the interval from 0430 to 0730 UT on 13 May 2001. The red line represents the electron gyrofrequency determined by the T96 magnetic field model. Numbers 1–12 denote the times when RPI active sounding mode obtained the X mode traces. The satellite orbit configuration is shown in the inserted panel.

the period the spacecraft was moving outward from the plasmasphere to the subauroral region, then to the northern polar cap. The red curve in the spectrogram denotes the electron cyclotron frequency f_{ce} calculated using the T96 model [*Tsyganenko*, 1995]. The orbital information, including the L shell, magnetic local time (MLT), radial distance in Earth radius (R_E), and the magnetic latitude (MLAT) are labeled below the abscissa, from which we can find that IMAGE was basically in the 0930–2130 local time meridian. In the spectrogram covering waves from 3 to 1000 kHz, the upper hybrid resonance (UHR) band with enhanced signal is clearly displayed. The frequency in the center of the UHR band decreases from 615 kHz (at 0525 UT) to 31 kHz (at 0625 UT) with a sudden drop at 0604 UT, which is recognized as the plasmapause. An inner trough is seen in the plasmasphere from 0546 UT to 0554 UT. The identification of the plasmapause is supported by the fact that inside the plasmasphere there are no (or very weak) waves detected in the frequency range between the local electron cyclotron frequency and lower cutoff frequency of the UHR band. Meanwhile beyond the nominal plasmapause exits nonthermal continuum emission which is believed to represent a broadband electromagnetic wave that propagates back and forth between the plasmapause and magnetopause [e.g., *Gurnett and Shaw*, 1973; *Kurth et al.*, 1981].

[10] With this spectrogram, the in situ electron densities are derived from the lower-frequency cutoff of the UHR band [e.g., *Mosier et al.*, 1973; *Benson et al.*, 2004] and presented in Figure 2 as the black dots. The blue dots denote the electron densities derived from the RPI active sounding measurements, which will be presented later. Figures 2a and 2b show the electron densities as functions of universal time and L shell, respectively. The electron density decreases gradually from 4737 to 1967 cm^{-3} in the interval of 0525–0544 UT. Then a density trough, highlighted with the shaded area, was encountered by IMAGE, when the density dropped to 255 cm^{-3} at 0552 UT, more than a factor of 3 lower compared to the density just outside the trough at 0556 UT. Beyond the outer boundary of this trough, IMAGE entered the outer plasmasphere. This segment of the IMAGE observations lasted from 0556 to 0602 UT when a typical plasmapause feature was encountered, extending from L = ~3.65 to L = ~3.90. At the plasmapause, the electron density dropped suddenly from 294 to 49 cm^{-3}, about a factor of 6 decreases over a region of ~0.25 R_E. Outside the plasmapause, i.e., in the plasmatrough, the electron density again decreased gradually from 49 to 13 cm^{-3} at 0625 UT when the UHR band became less clearly identifiable. From Figure 2b, the inner density trough extends from L = 2.3 to L = 3.0 along the orbit, i.e., a width of 0.7 R_E. The width and density drop in this case are consistent with that observed by *Carpenter et al.* [2000]: widths ranging from $\Delta L \sim 0.5$ to $\Delta L \sim 1.5$ and density drop by a factor of ~2–5. It has also been postulated by *Carpenter et al.* [2000] that the density trough may extend down to

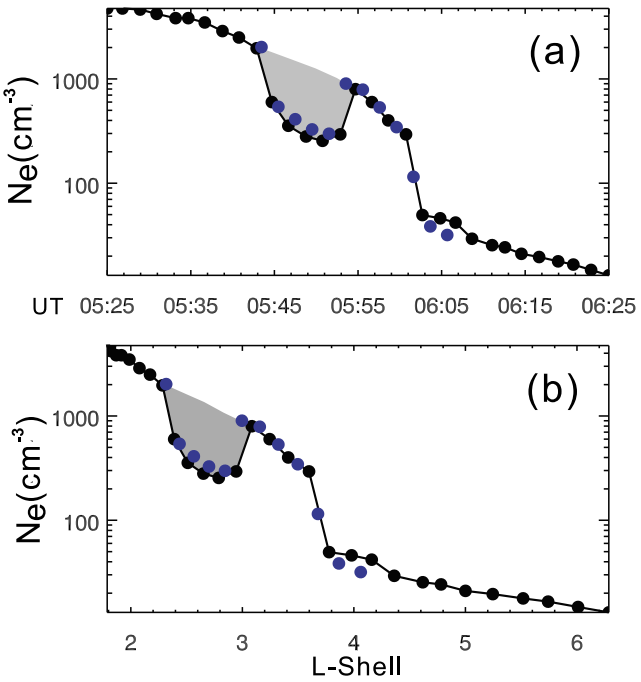

Figure 2. Electron density profiles as functions of (a) the universal time and (b) L shell. Black dots denote the densities deduced from the UHR band in the dynamic spectrogram shown in Figure 1, while blue dots denote the densities derived from the RPI active measurements. The shaded region highlights the density trough inside the plasmasphere.

ionosphere altitudes. The actual extent, however, could not be determined directly from the in situ observations. In the following, we examine the spatial extent of this density trough along the geomagnetic field.

3.2. IMAGE RPI Sounding Measurements

[11] The RPI active sounding measurements provided a set of successive X mode traces from 0544 to 0606 UT, covering both the inner trough and plasmapause. We marked the locations where the traces were observed with the numbers 1–12 in the dynamic spectrogram in Figure 1. The locations and times of those traces are listed in Table 1. As an example, Figure 3 shows the plasmagram obtained by the RPI active sounding mode at 0546 UT, when IMAGE was located in the inner density trough labeled with number 2 in Figure 1. Intensities of received signals as a function of virtual range and frequency are displayed. The simultaneous orbit configuration of IMAGE is also shown in the inserted panel, in which the red dot represents the satellite's location and the dipole field line denotes $L = 3.7$, corresponding to the location of the plasmapause (see Figure 2b); thus, the satellite was located inside the plasmasphere. In Figure 3, a trace with enhanced signals extends from ~239 to ~440 kHz. There are also several resonances detected, including the plasma oscillation which is shown as enhanced signals extending vertically at $f_{pe} \sim 204.6$ kHz, the upper hybrid resonance at $f_{uh} \sim 214.4$ kHz, and the electron cyclotron harmonics indicated by the enhanced signals at $4f_{ce} \sim 255.6$ kHz and $5f_{ce} \sim 319.5$ kHz. Because of the higher starting frequency of the RPI sounding program at that time, the electron cyclotron frequency f_{ce} is out of range. Considering relationship between these frequencies $f_x = \frac{f_{ce}}{2} + \frac{1}{2}\sqrt{f_{ce}^2 + 4f_{pe}^2}$ and $f_{uh} = \sqrt{f_{ce}^2 + f_{pe}^2}$, the trace is recognized as the X mode [e.g., *Reinisch et al.*, 2001; *Nsumei et al.*, 2003; *Tu et al.*, 2005] formed by echoes propagating along the magnetic field. The X mode trace is scaled by a black curve shown in Figure 3.

[12] By applying the inversion algorithm developed by *Huang et al.* [2004] to the scaled traces on 12 successive plasmagrams, we obtain 12 electron density profiles, which are displayed in Figure 4 as functions of magnetic latitude. The field-aligned density profiles cover the inner trough region. Specifically, profile 1 is at the inner plasmasphere, profiles 2–5 are inside the density trough (blue lines), profiles 6–9 are at the outer plasmasphere, profile 10 is at the plasmapause or plasmasphere boundary layer (PBL) [*Carpenter and Lemaire*, 2004], and profiles 11–12 are in the plasmatrough. It should be mentioned that density profile 10 consists of the electron density distributions in both Southern and Northern hemispheres. Other density profiles, however, include only the electron density distributions in the local (northern) hemisphere because of the limited top virtual range of the measurement program. Density profiles 1–9 are derived from the plasmagrams recorded using the program 35 with virtual ranges up to 4.5 R_E. The trace from the conjugate hemisphere, if any, would be out of range. Profile 10 is obtained from the plasmagram recorded using the program 34 with virtual ranges up to 8.2 R_E, greater than the virtual range of the conjugate trace (~6.5 R_E). Therefore, we obtain the density profiles for both the local and conjugate hemispheres. Although density profiles 11–12 are derived from the measurements using the program 34, the traces from the conjugative hemisphere are too diffuse to be scaled so that the conjugate density profiles cannot be derived. The circle on each density profile represents the local electron density determined by the vertical resonance line of f_{pe} in the plasmagram. These local electron densities are also shown in Figure 2 (blue dots), as a comparison with the passive measurements. We find the electron densities derived from the active and passive measurements basically match each other, where the small differences may result from measurement errors (<10% uncertainty for both measurements in the present case [*Benson et al.*, 2004; *Tu et al.*, 2005]).

[13] Using the measured field-aligned profiles, we construct a 2-D density image in the meridian traversed by IMAGE, as shown in Figure 5. Because the IMAGE pass lasts for only ~22 min, the image can be considered to be roughly within the same local time sector (MLT ~ 2130). The PBL is found located at $L \sim 3.68$ (indicated by the thick black field line). Inside the plasmasphere, there is a low-density region or density trough between $L \sim 2.32$ to $L \sim 3.00$. It extends along the magnetic field lines from the IMAGE orbit to about 41° MLAT and possibly to the ionosphere.

3.3. DMSP-F15 Observations

[14] In order to determine whether the density trough really extends to the ionosphere altitudes, we examine the DMSP-F15 observations at the topside ionosphere. Because the DMSP-F15 satellite circled the Earth near the meridian of 0930–2130 MLT, it coincided with the IMAGE's orbit very well, which was also in the ~2130 meridian during the period of 0544–0606 UT when the IMAGE RPI sounding mea-

Table 1. Times and Locations of Field-Aligned Density Profiles[a]

Profile		UT	*L* shell
1	IPS	0544	2.32
2	IDT	0546	2.44
3		0548	2.56
4		0550	2.70
5		0552	2.84
6	OPS	0554	3.00
7		0556	3.16
8		0558	3.32
9		0600	3.50
10	PBL	0602	3.68
11	PT	0604	3.87
12		0606	4.06

[a]Derived from RPI active sounding measurements on 13 May 2001 in different regions including the inner plasmasphere (IPS), inner density trough (IDT), outer plasmasphere (OPS), plasmasphere boundary layer (PBL), and plasmatrough (PT).

surements were made. These two satellites crossed roughly the same field lines with one at high altitudes and the other at low altitudes, providing coordinated observations of the density trough. Figure 6 shows the measurements from DMSP-F15 during the interval 0550–0620 UT on 13 May 2001, i.e., almost simultaneous observations with the IMAGE measurements. In Figures 6a–6f, the densities of total ions N_i, He^+ and H^+ ions, the precipitating electron and ion energy flux, and the dipole *L* shell are exhibited. Parameters at the bottom provide information about the DMSP-F15 orbit, including the *L* value, magnetic latitude (MLAT), magnetic local time (MLT), and the altitude (ALT). The leftmost dashed vertical line marks the boundary between the cold and hot plasma (see Figures 6d and 6e). It also represents the inner boundary of the light ion trough (LIT) at the topside ionosphere [e.g., *Lemaire*, 2001; *Anderson et al.*, 2008]. This boundary was located at $L \sim 3.9$ (see Figures 6f), slightly poleward of the PBL at high altitude, which was observed by IMAGE RPI at $L \sim 3.68$. This is a typical feature of the location of the LIT as revealed by *Anderson et al.* [2008], who showed that the LIT boundary observed by the DMSP is usually about 0.5 *L* farther poleward compared to the PBL at high altitudes. The corresponding plasmasphere at high altitudes is on the right of this boundary. It is important to note that an inner trough in the light ion (H^+ and He^+) densities (shadowed region) is observed on the right of the LIT boundary (Figures 6b and 6c). It extends from $L \sim 2.2$ to $L \sim 3.0$ (see Figure 6f). The location of the inner light ion density trough coincides well with the inner density trough (extending from $L \sim 2.32$ to $L \sim 3.00$) observed by IMAGE RPI at high altitudes. Note that the DMSP-F15 crossed the inner light ion density trough during the period of 0608–0610 UT, very

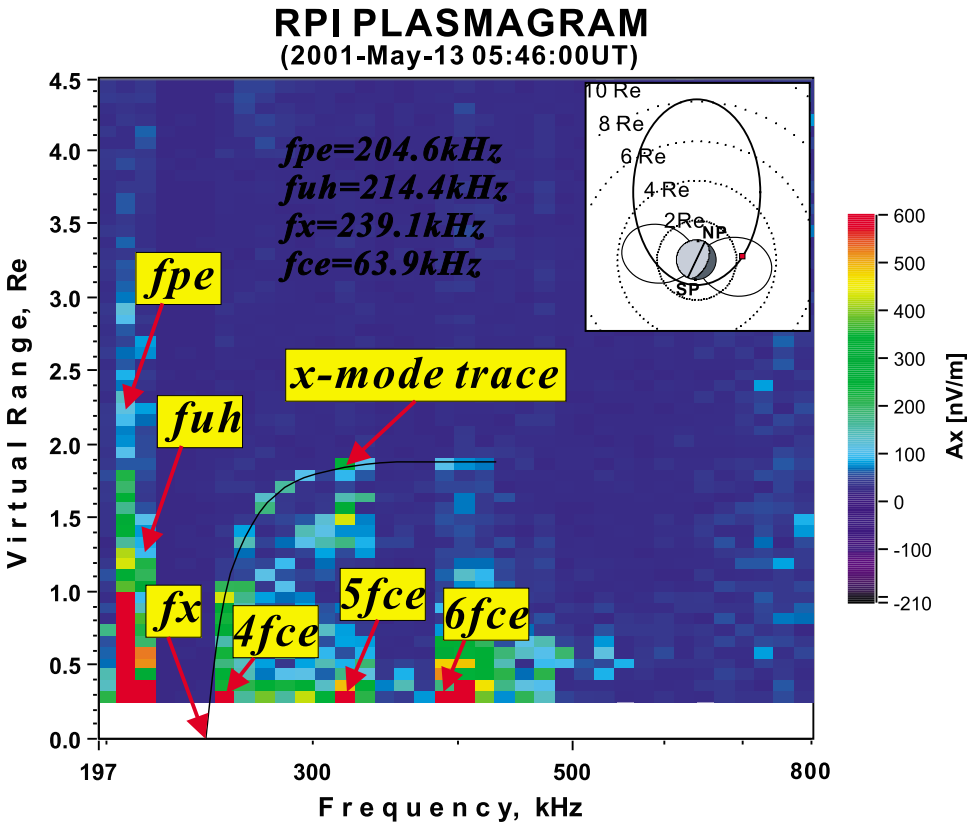

Figure 3. A plasmagram recorded by RPI active sounding measurements at 0546 UT on 13 May 2001, when IMAGE was locating inside the inner density trough. Signal amplitudes are shown as functions of frequency and time delay expressed in terms of virtual range. A trace, formed from X mode echoes, extends from ~239 to ~440 kHz. Local electron plasma, upper hybrid resonance, and also fourth to sixth harmonics of the electron cyclotron resonance are seen as enhanced vertical lines. The inset displays the simultaneous orbit configuration of IMAGE, represented as the red dot.

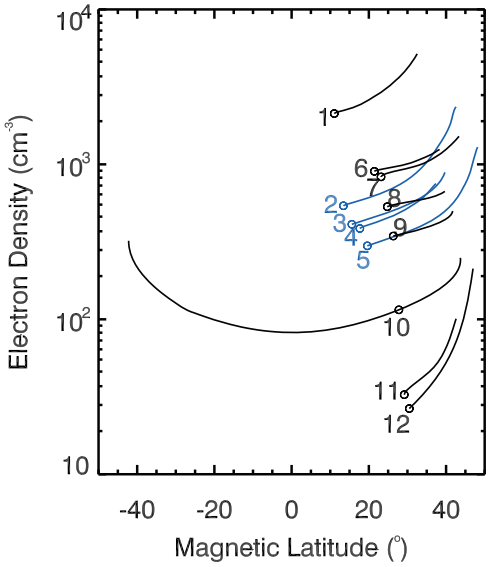

Figure 4. Field-aligned electron density profiles derived from the RPI active sounding measurements as functions of magnetic latitude in the interval from 0544 to 0606 UT on 13 May 2001. The locations where they are derived correspond roughly to those numbered in Figure 1. The blue lines indicate the density profiles obtained in the inner density trough. Circles on the measured density profiles represent the local electron densities obtained from the local plasma resonances.

close to the time period of ~0546 to ~0552 UT when IMAGE traversed the inner density trough at high altitude. The magnetic local time (~2300 MLT) of the DMSP-F15 crossing of the inner light ion density trough is also close to that of the IMAGE crossing of the plasmaspheric density trough (~2130 MLT). Therefore, the inner light ion density trough observed by the DMSP-F15 corresponds to the plasmaspheric density trough observed by RPI and is its extension to the topside ionosphere along the magnetic field lines. In other words, the density trough inside the plasmasphere, which has been shown by the RPI sounding measurements to be field aligned (Figure 5), quite possibly extends to the topside ionosphere, as conjectured by *Carpenter et al.* [2000]. Here we notice that the total ion density (see Figure 6a) does not show the trough signature. This is because at the DMSP altitude the dominant ion species is O^+ so that the effect of the low H^+ density is not observable in the total density.

3.4. IMAGE EUV Observations

[15] One issue relevant to the present observations is whether the observed density trough is related to the low-density channel between the main body of the plasmasphere and plasmaspheric plume. We first examine the geomagnetic conditions for the existence of the plasmaspheric plume. Shown in Figure 7 are, from top to bottom, the D_{st} index recorded from 6 to 13 May 2001 (Figure 7a), the K_p, D_{st}, IMF B_z, and the solar wind ram pressure P_{sw} in the interval from 1200 UT on 12 May to 1200 UT on 13 May 2001 (Figures 7b–7e). The two vertical lines in Figures 7b–7e indicate the period when the inner density trough was observed, i.e., from ~0546 to ~0552 UT on 13 May. As can be seen, prior to the RPI observations of the density trough, the D_{st} index could be less than −40 (Figure 7c) and the K_p index could be in excess of 5 (Figure 7b) on 12 May. The IMF B_z was primarily southward, and the solar wind dynamic pressure varied dramatically at sometimes (Figures 7d–7e). When focusing on the D_{st} index several days ago (Figure 7a), we find the D_{st} index varied suddenly from positive to negative on 7 May. After a little recovery on 8 May, it then reached the minimum value (~−80 nT) on 10 May. This D_{st} index, from 7 to 13 May, increased and decreased repeatedly, leading to a complicated geomagnetic condition. The observed density trough structure appeared in the aftermath of periods of enhanced geomagnetic activity.

[16] Under this geomagnetic condition, a plume feature was observed by the IMAGE EUV imager, as shown in Figure 8. Figure 8a displays a global image of the plasmasphere taken at 0749 UT on 13 May 2001 without any background subtraction, which is the first clear global image after IMAGE moved out of the plasmasphere. In Figure 8a, the dashed circle indicates the Earth, while the white squares represent the plasmapause, which is determined by the sharp drop of the abundance of He^+ that is expressed by the haze around the Earth [*Spasojević et al.*, 2003]. Although the plasmapause is usually defined by the density of H^+ and the ratio of He^+ to H^+ varies from time to time [*Craven et al.*, 1997], *Goldstein et al.* [2003] showed the feasibility to identify the plasmapause by the He^+ density based on a statistical study. The arrowhead indicates the Sun direction, against which the Earth's shadow is clearly seen. A plasmaspheric plume is also seen in the premidnight sector. To remove the perspective distortion of the image caused by the changing distance and view angle, the plasmapause is mapped to the equatorial plane as represented by the dots in Figure 8b. The mapping principle is based on the fact that the

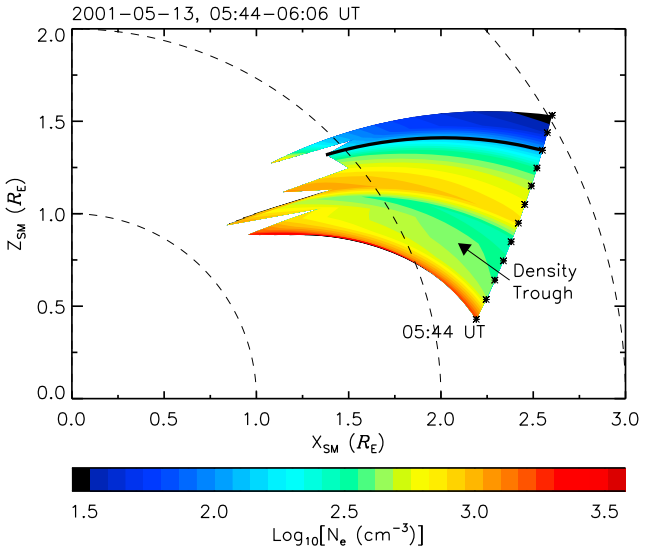

Figure 5. 2-D electron density images from $L \sim 2.32$ to $L \sim 4.06$ in the sector of MLT = ~2130. The density image is constructed using the profiles in Figure 4. The stars on the orbit segment indicate the locations from which the field-aligned density profiles were measured. The thick black line expresses the location of plasmapause. A density trough is seen in the region from $L \sim 2.32$ to $L \sim 3.00$.

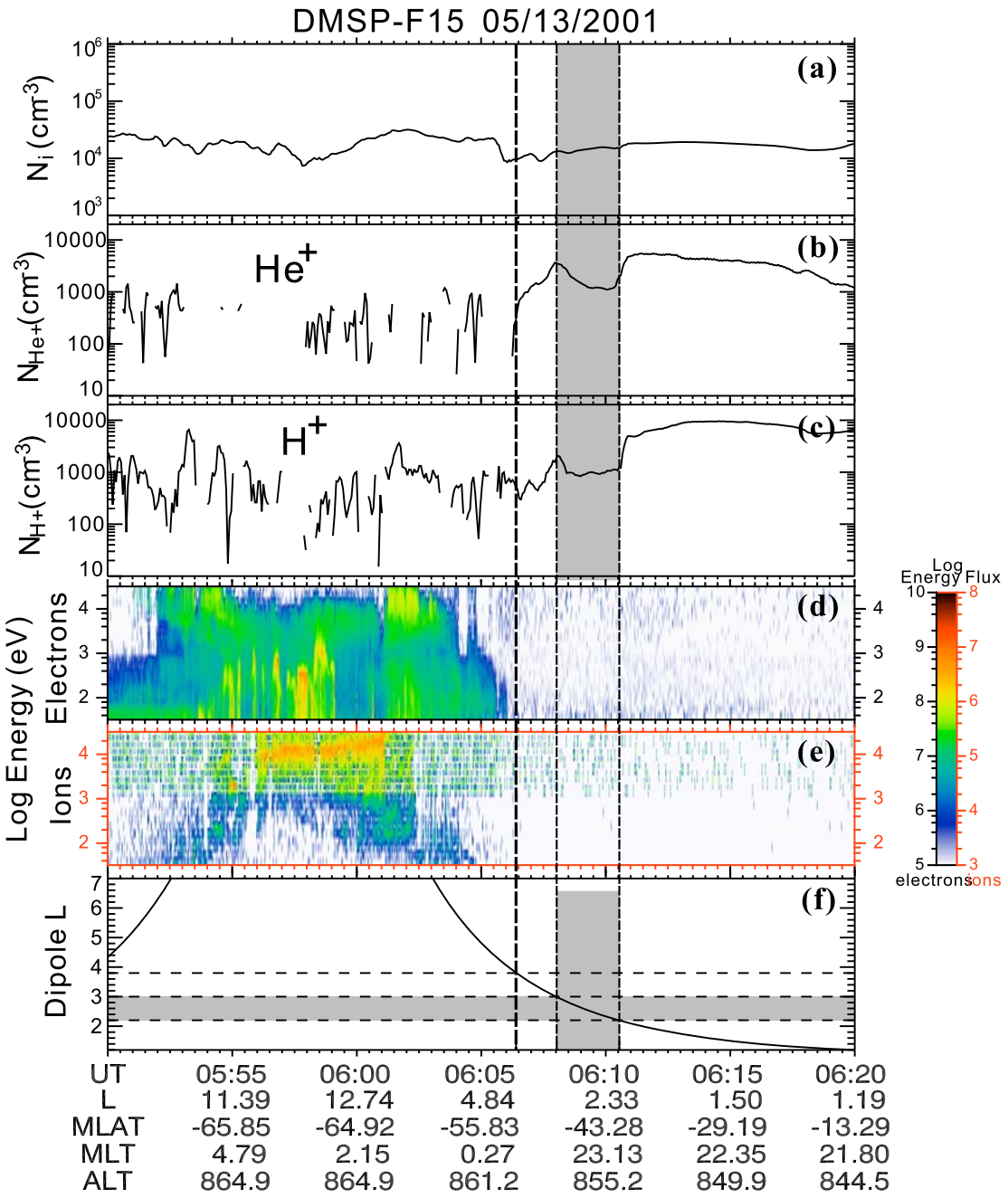

Figure 6. Measurements of (a) the total ion density, (b) He^+ density, (c) H^+ density, (d) the precipitating electron and (e) ion energy flux spectra, and (f) the dipole *L* shell along DMSP-F15 satellite orbit at ~850 km altitude (ALT) from 0550 to 0620 UT on 13 May 2001. The shaded region indicates a density trough in the profiles of light ions (He^+ and H^+). The leftmost vertical dashed line represents the boundary of the LIT, which roughly corresponds to the plasmapause at high altitudes.

integrated density of He^+ along the sight line of camera is mainly contributed from the minimum *L* shell when the sight line is tangent to the plasmapause [*Goldstein et al.*, 2003]. A dipole geomagnetic field is assumed during the mapping process. The uncertainty that comes from the manual selection of the He^+ edge in the image (see white squares in Figure 8a) is about 0.2–0.8 R_E depending on the sharpness of the edge [*Goldstein et al.*, 2003]. In Figure 8b, the dayside is on the left. We notice that the EUV image was taken 2 h after the RPI measurements shown in Figure 4. If the density trough and other plasmaspheric structures corotated with the Earth, the image in Figure 8a corresponds to the structures at 0549 UT when it is rotated by 30° westward, which is included in Figure 8b. Here it is necessary to mention that there usually exists a lag of 3%–15% in the corotation of the plasmasphere compared to the rotation of the Earth [e.g., *Burch et al.*, 2004; *Gallagher et al.*, 2005; *Galvan et al.*, 2008]. This lag corresponds to an uncertainty of 1°–5°, a

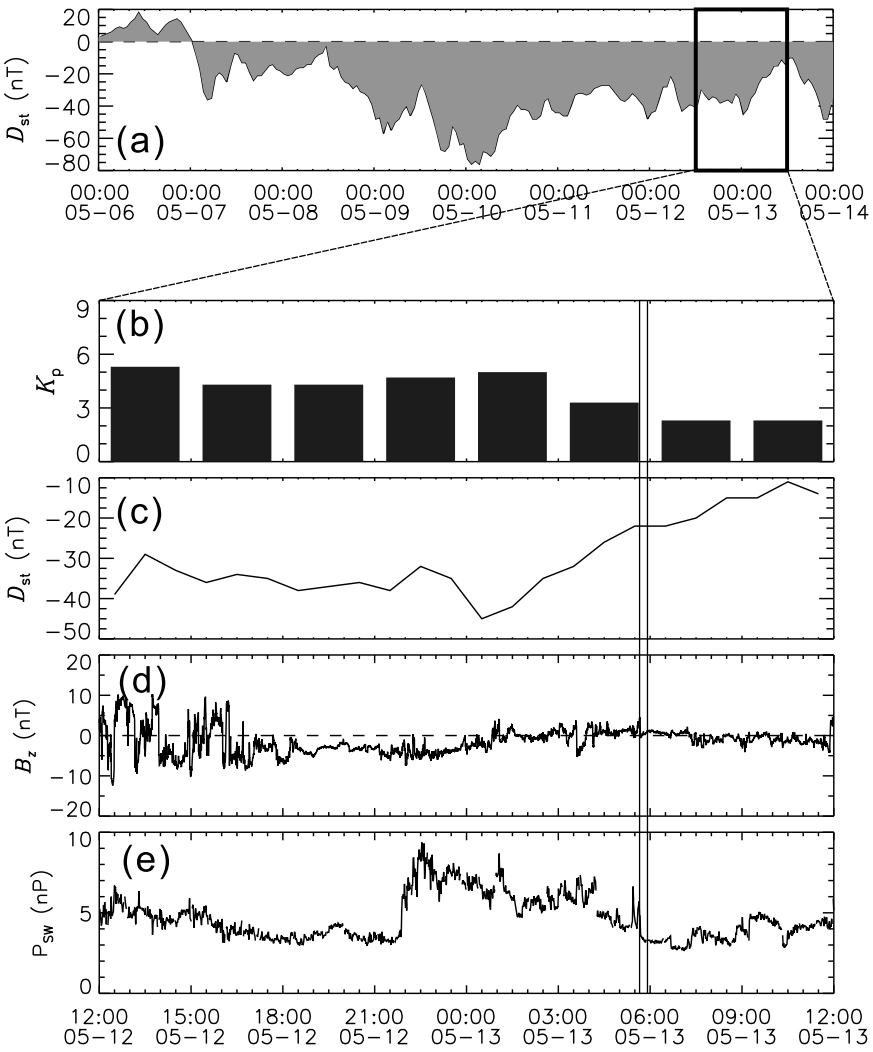

Figure 7. (a) D_{st} index recorded from 6 to 13 May in the year 2001. (b–e) K_p, D_{st}, IMF B_z, and the solar wind ram pressure P_{sw} in the interval from 1200 UT on 12 May 2001 to 1200 UT on 13 May 2001. The two vertical lines indicate the period when the inner density trough was observed.

negligible value, when we rotate the plasmaspheric structure to 2 h ago as shown in Figure 8b. The arrowhead represents the sector of MLT ~ 2130, which was roughly the MLT sector of the IMAGE orbit from 0544 to 0606 UT. On the arrow, the black bar from L ~ 2.3 to L ~ 3.0 denotes the location of the inner density trough observed by the RPI. As can be seen, the plasmapause determined by the EUV image along the IMAGE orbit is at L ~ 3.7, very consistent with the RPI observation, which is at L ~ 3.68. This also confirms that the rotation of 30° westward of the plasmasphere is reasonable because the plasmapause radial distance is a function of MLT. We see that the density trough observed by RPI was located inside the plasmasphere. It was therefore not the low-density channel between the plasmaspheric plume and the main body of the plasmasphere.

[17] In Figure 8a, we see that embedded inside the plasmaspheric plum there is a channel with lower density compared to its surrounding region. The channel locates at L = ~3 but is more than 1 h away from the density trough in terms of magnetic local time. Therefore, the density trough observed by the IMAGE RPI is not related to this channel inside the plasmaspheric plume, even with the rotation lag of the plasmaspheric plume taken into account.

4. Summary

[18] The present study presents the coordinated observations of a density trough using the measurements from the IMAGE RPI and EUV and the DMSP-F15 satellite. The density trough was located from L = ~ 2.3 to ~3.0 and was crossed by the IMAGE satellite at about 2130 MLT. The electron density within the trough was depleted up to 1/3 of that in the surrounding regions. The density trough was detected during the period of enhanced geomagnetic activity in terms of K_p and D_{st} index. All these features are consistent with those of the density troughs observed previously using in situ measurements [e.g., *Horwitz et al.*, 1990; *Carpenter et al.*, 2000].

[19] With the aid of the global plasmasphere images obtained by the IMAGE EUV, we are able to determine that

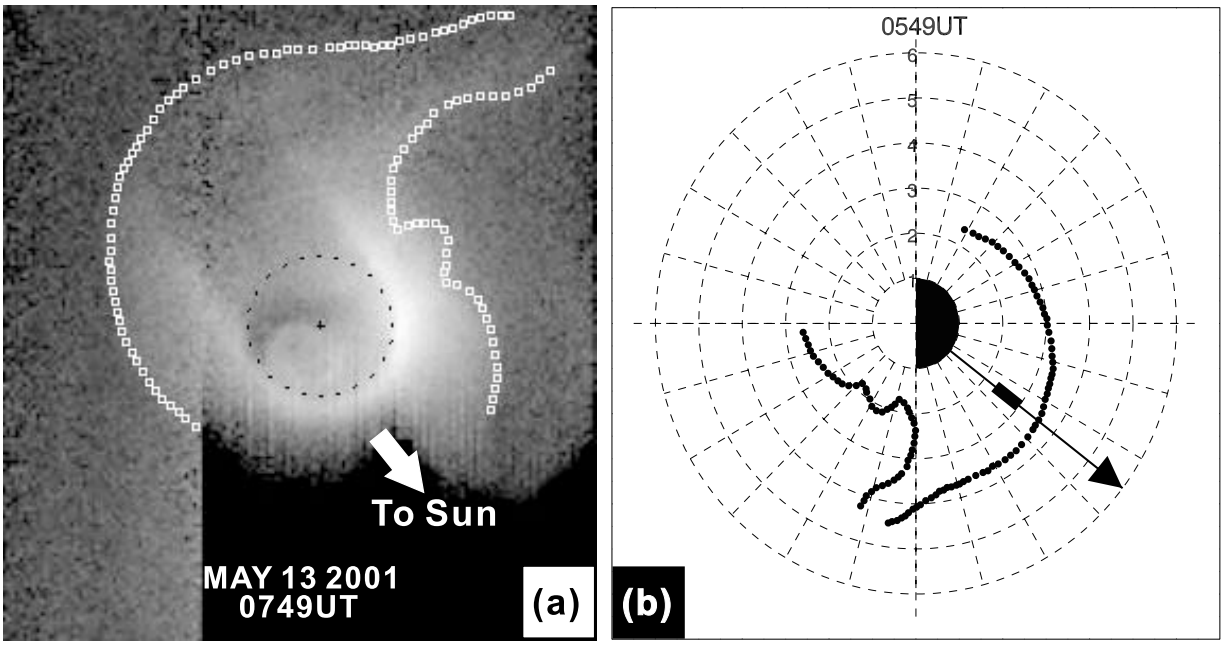

Figure 8. (a) A global image of the plasmasphere without background subtraction, showing a plasmaspheric plume in the premidnight sector, taken by the IMAGE EUV on 13 May 2001 at 0749 UT when the satellite just moved out of the plasmasphere. The dashed circle indicates the Earth, while white squares represent the plasmapause determined by the sharp drop of He^+ emission brightness. (b) 30° clockwise rotation of the global plasmapause in Figure 8a, i.e., against the direction of Earth's rotation. It represents the global shape of the plasmasphere at 0549 UT (2 h before Figure 8a) assuming the plasmasphere is fully corotated with the Earth. Black dots denote the location of plasmapause that has been mapped to the equatorial plane. The arrow indicates the magnetic local sector of the IMAGE orbit near 0549 UT, on which the black bar indicates the location of the inner density trough observed by the RPI.

the observed density trough is a structure embedded inside the plasmasphere rather than the low-density channel between the main body of the plasmasphere and plasmaspheric plume. The unique field-aligned density profiles derived from the RPI sounding measurements for the first time display the spatial extent of the density trough in the plasmasphere. It is shown that the observed density trough extends from the IMAGE orbit to at least 41° MLAT along the field lines. The coordinated DMSP-F15 observations further illustrate that a light ion density trough existed simultaneously with the plasmasphere density trough along the same field lines, indicating that the plasmasphere density trough extends from the plasmasphere to the ionosphere as conjectured by *Carpenter et al.* [2000].

[20] Our observations revealed the spatial extent of the inner density trough along the field lines. How such density troughs inside the main body of the plasmasphere are formed and sustained, however, is still an open question. The simulations by *Ober et al.* [1997] using a dynamic global core plasma model suggested that the density trough was resulted from the subauroral ion drift (SAID). We are, however, not able to definitely establish relation of the observed density trough to any SAIDs with the available observational data set. Investigations on more cases are needed to address this issue.

[21] **Acknowledgments.** This work was supported by NASA grants NNX07AG38G and NNX08AF31G and NSF grant ATM-0902965 to the University of Massachusetts Lowell. Work by J. B. Cao was supported by NSFC grant 40931054, 973 Program 2006CB806305 and the Specialized Research Fund of State Key Laboratories of Space Weather in China. We gratefully acknowledge the Center for Space Sciences at the University of Texas at Dallas and the U. S. Air Force for providing the DMSP thermal plasma data. K_p and D_{st} indices were obtained through the Website of the World Data Center for Geomagnetism, Kyoto. ACE spacecraft data were obtained through the CDAWeb (http://cdaweb.gsfc.nasa.gov).

[22] Robert Lysak thanks James Burch and another reviewer for their assistance in evaluating this paper.

References

Adrian, M. L., D. L. Gallagher, and L. A. Avanov (2004), IMAGE EUV observation of radially bifurcated plasmaspheric features: First observations of a possible standing ULF waveform in the inner magnetosphere, *J. Geophys. Res.*, *109*, A01203, doi:10.1029/2003JA009974.

Anderson, P. C., D. L. Carpenter, K. Tsuruda, T. Mukai, and F. J. Rich (2001), Multisatellite observations of rapid subauroral ion drifts (SAID), *J. Geophys. Res.*, *106*(A12), 29,585–29,599.

Anderson, P. C., W. R. Johnston, and J. Goldstein (2008), Observations of the ionospheric projection of the plasmapause, *Geophys. Res. Lett.*, *35*, L15110, doi:10.1029/2008GL033978.

Benson, R. F., P. A. Webb, J. L. Green, L. Garcia, and B. W. Reinisch (2004), Magnetospheric electron densities inferred from upper-hybrid band emissions, *Geophys. Res. Lett.*, *31*, L20803, doi:10.1029/2004GL020847.

Burch, J. L., et al. (2001), Views of Earth's magnetosphere with the IMAGE satellite, *Science*, *91*(5504), 619–624.

Burch, J. L., J. Goldstein, and B. R. Sandel (2004), Cause of plasmasphere corotation lag, *Geophys. Res. Lett.*, *31*, L05802, doi:10.1029/2003GL019164.

Burke, W. J., A. G. Rubin, N. C. Maynard, L. C. Gentile, P. J. Sultan, F. J. Rich, O. de La Beaujardière, C. Y. Huang, and G. R. Wilson (2000), Ionospheric disturbances observed by DMSP at middle to low latitudes during the magnetic storm of June 4–6, 1991, *J. Geophys. Res.*, *105*, 18,391–18,405.

Cao, J. B., et al. (2005), First results of low frequency electromagnetic wave detector of TC-2/Double Star program, *Ann. Geophys.*, *23*, 2803–2811.

Carpenter, D. L., and J. Lemaire (1997), Erosion and recovery of the plasmasphere in the plasmapause region, *Space Sci. Rev.*, *80*, 153–179.
Carpenter, D. L., and J. Lemaire (2004), The plasmasphere boundary layer, *Ann. Geophys.*, *22*, 4291–4298.
Carpenter, D. L., R. R. Anderson, W. Calvert, and M. B. Moldwin (2000), CRRES observations of density cavities inside the plasmasphere, *J. Geophys. Res.*, *105*, 23,323–23,338.
Craven, P. D., D. L. Gallagher, and R. H. Comfort (1997), Relative concentration of He^+ in the inner magnetosphere as observed by the DE 1 retarding ion mass spectrometer, *J. Geophys. Res.*, *102*, 2279–2289.
Dandouras, I., J. Cao, and C. Vallat (2009), Energetic ion dynamics of the inner magnetosphere revealed in coordinated Cluster-Double Star observations, *J. Geophys. Res.*, *114*, A01S90, doi:10.1029/2007JA012757.
Darrouzet, F., et al. (2009), Plasmaspheric density structures and dynamics: Properties observed by the CLUSTER and IMAGE missions, *Space Sci. Rev.*, *145*, 55–106, doi:10.1007/s11214-008-9438-9.
De Keyser, J., M. Roth, and J. Lemaire (1998), The magnetospheric driver of subauroral ion drifts, *Geophys. Res. Lett.*, *25*, 1625–1628.
Fu, H. S., J. Tu, P. Song, J. B. Cao, B. W. Reinisch, and B. Yang (2010), The nightside-to-dayside evolution of the inner magnetosphere: Imager for Magnetopause-to-Aurora Global Exploration Radio Plasma Imager observations, *J. Geophys. Res.*, *115*, A04213, doi:10.1029/2009JA014668.
Fung, S. F., and J. L. Green (2005), Modeling of field-aligned radio echoes in the plasmasphere, *J. Geophys. Res.*, *110*, A01210, doi:10.1029/2004JA010658.
Gallagher, D. L., M. L. Adrian, and M. W. Liemohn (2005), Origin and evolution of deep plasmaspheric notches, *J. Geophys. Res.*, *110*, A09201, doi:10.1029/2004JA010906.
Galvan, D. A., M. B. Moldwin, and B. R. Sandel (2008), Diurnal variation in plasmaspheric He^+ inferred from extreme ultraviolet images, *J. Geophys. Res.*, *113*, A09216, doi:10.1029/2007JA013013.
Goldstein, J., M. Spasojević, P. H. Reiff, B. R. Sandel, W. T. Forrester, D. L. Gallagher, and B. W. Reinisch (2003), Identifying the plasmapause in IMAGE EUV data using IMAGE RPI in situ steep density gradients, *J. Geophys. Res.*, *108*(A4), 1147, doi:10.1029/2002JA009475.
Gurnett, D. A., and R. R. Shaw (1973), Electromagnetic radiation trapped in the magnetosphere above the plasma frequency, *J. Geophys. Res.*, *78*, 8136–8149.
Hairston, M. R., and R. A. Heelis (1990), Model of the high-latitude ionospheric convection pattern during southward interplanetary magnetic field using DE 2 data, *J. Geophys. Res.*, *95*, 2333–2343.
Horwitz, J. L., R. H. Comfort, and C. R. Chappell (1990), A statistical characterization of plasmasphere density structure and boundary locations, *J. Geophys. Res.*, *95*, 7937–7947.
Huang, X., B. W. Reinisch, P. Song, J. L. Green, and D. L. Gallagher (2004), Developing an empirical density model of the plasmasphere using IMAGE/RPI observations, *Adv. Space Res.*, *33*, 829–833.
Kurth, W. S., D. A. Gurnett, and R. R. Anderson (1981), Escaping nonthermal continuum radiation, *J. Geophys. Res.*, *86*, 5519–5531.
Lemaire, J. F. (2001), The formation of the light-ion trough and peeling off the plasmasphere, *J. Atmos. Terr. Phys.*, *63*, 1285–1291.
Lemaire, J. F., and K. I. Gringauz (1998), *The Earth's plasmasphere*, 372 pp., Cambridge Univ. Press, Cambridge.
Moldwin, M. B. (1997), Outer plasmaspheric plasma properties: What we know from satellite data, *Space Sci. Rev.*, *80*, 181–198.
Mosier, S. R., M. L. Kaiser, and L. W. Brown (1973), Observations of noise bands associated with the upper hybrid resonance by the Imp 6 radio astronomy experiment, *J. Geophys. Res.*, *78*, 1673–1679.
Nishida, A. (1966), Formation of plasmapause, or magnetospheric plasma knee, by the combined action of magnetospheric convection and plasma escape from the tail, *J. Geophys. Res.*, *71*, 5669–5679.
Nsumei, P. A., X. Huang, B. W. Reinisch, P. Song, V. M. Vasyliunas, J. L. Green, S. F. Fung, R. F. Benson, and D. L. Gallagher (2003), Electron density distribution over the northern polar region deduced from IMAGE/radio plasma imager sounding, *J. Geophys. Res.*, *108*(A2), 1078, doi:10.1029/2002JA009616.
Ober, D. M., J. L. Horwitz, and D. L. Gallagher (1997), Formation of density troughs embedded in the outer plasmasphere by subauroral ion drift events, *J. Geophys. Res.*, *102*, 14,595–14,602.
Reinisch, B. W., et al. (2000), The radio plasma imager investigation on the IMAGE spacecraft, *Space Sci. Rev.*, *91*, 319–359.
Reinisch, B. W., X. Huang, P. Song, G. S. Sales, S. F. Fung, J. L. Green, D. L. Gallagher, and V. M. Vasyliunas (2001), Plasma density distribution along the magnetospheric field: RPI observations from IMAGE, *Geophys. Res. Lett.*, *28*(24), 4521–4524.
Reinisch, B. W., X. Huang, P. Song, J. L. Green, S. F. Fung, V. M. Vasyliunas, D. L. Gallagher, and B. R. Sandel (2004), Plasmaspheric mass loss and refilling as a result of a magnetic storm, *J. Geophys. Res.*, *109*, A01202, doi:10.1029/2003JA009948.
Sandel, B. R., et al. (2000), The extreme ultraviolet (EUV) imager investigation for the IMAGE mission, *Space Sci. Rev.*, *91*, 197–242.
Sandel, B. R., R. A. King, W. T. Forrester, D. L. Gallagher, A. L. Broadfoot, and C. C. Curtis (2001), Initial results from the IMAGE extreme ultraviolet imager, *Geophys. Res. Lett.*, *28*(8), 1439–1442.
Sandel, B. R., J. Goldstein, D. L. Gallagher, and M. Spasojević (2003), Extreme ultraviolet imager observations of the structure and dynamics of the plasmasphere, *Space Sci. Rev.*, *109*(1–4), 25–46, doi:10.1023/B:SPAC.0000007511.47727.5b.
Spasojević, M., J. Goldstein, D. L. Carpenter, U. S. Inan, B. R. Sandel, M. B. Moldwin, and B. W. Reinisch (2003), Global response of the plasmasphere to a geomagnetic disturbance, *J. Geophys. Res.*, *108*(A9), 1340, doi:10.1029/2003JA009987.
Taylor, H. A., Jr., J. M. Grebowsky, and W. J. Walsh (1971), Structured variations of the plasmapause: Evidence of a corotating plasma tail, *J. Geophys. Res.*, *76*, 6806–6814.
Tsyganenko, N. A. (1995), Modeling the Earth's magnetospheric magnetic field confined within a realistic magnetopause, *J. Geophys. Res.*, *100*, 5599–5612.
Tu, J., P. Song, B. W. Reinisch, X. Huang, J. L. Green, H. U. Frey, and P. H. Reiff (2005), Electron density images of the middle- and high-latitude magnetosphere in response to the solar wind, *J. Geophys. Res.*, *110*, A12210, doi:10.1029/2005JA011328.

J. B. Cao, State Key Laboratory for Space Weather/CSSAR, No. 1 Nanertiao, Zhongguancun, Haidian District, Beijing, 100190, China.
H. S. Fu, B. W. Reinisch, P. Song, J. Tu, and B. Yang, Center for Atmospheric Research, University of Massachusetts Lowell, 600 Suffolk St, 3rd Floor, Lowell, MA 01854, USA. (huishanf@gmail.com)
D. L. Gallagher, NASA Marshall Space Flight Center, Huntsville, AL 35812, USA.